Proceedings of the Institute of Acoustics

ADAPTIVE FEEDBACK CONTROL OF SUN ROOF FLOW OSCILLATIONS

I.M. Stothers (1), T.J. Saunders (1), A.M. McDonald (1) and S.J. Elliott (2)

(1) Lotus Engineering, Norwich, NR14 8EZ
(2) Institute of Sound and Vibration Research, University of Southampton, Southampton SO9 5NH

1. INTRODUCTION

Engine noise and wind noise are familiar problems in the automotive industry, but noise generated from an open sun roof is perhaps less well documented. The effect can be understood by the experiment of blowing air across the open top of a glass bottle which in turn produces a discrete tone. Energy from the blown air excites the acoustic modes within the cavity of the bottle so that the shear layer associated with the jet oscillates into and out of the bottle. The oscillation is similar to that produced in an organ pipe, as analysed by Fletcher and Rossing (1991), for example. Another analysis of a flow excited resonance is given by Nelson *et al* (1981, 1983), who also give references to earlier work in this area.

George (1989) provides an excellent review of vehicle aeroacoustics, including a discussion of the sources of noise caused by flow over a cavity. Two forms of noise are identified: broadband noise and tone noise, as illustrated in Figure 1. It is the tone noise caused by an unstable shear layer which we are principally concerned with in this paper. The problem often only occurs at critical speeds, at which the natural frequency of the shear layer is

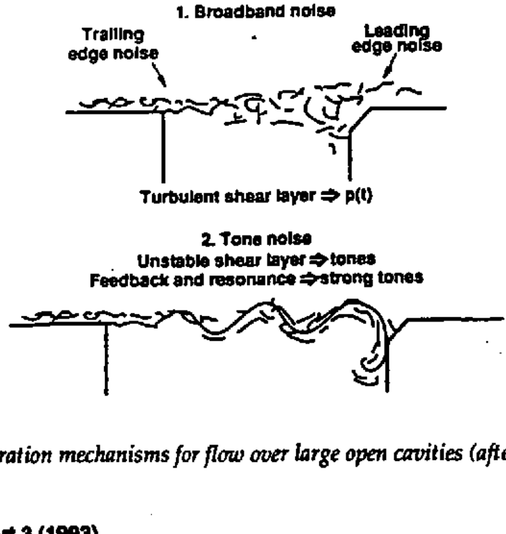

Figure 1. Noise generation mechanisms for flow over large open cavities (after George, 1989).

similar to an acoustic resonance frequency. Various methods of analysing and potentially controlling this noise in cars have been proposed by Bodger and Jones (1964) and Lackman (1989), for example. Such methods include smoothing the flow over the sunroof, or changing the natural frequency or damping of the system. This source of noise remains, however, a significant problem in a number of cars.

Our experience of one particular full-size motor car, revealed dramatic consequences of travelling at the critical speed while the sun roof was fully open. Gradually increasing road speed from stationary created a tremendously loud 24 Hz tone inside the passenger compartment. Generation occurred at a frequency consistent with the volume of the car cavity and the sun roof aperture size being excited by the air flow over the open aperture. By further increasing road speed the amplitude was reduced by passing through the resonance. Alternatively, a window could be opened fractionally to dampen the cavity, or the sun roof position could be adjusted to reduce the area and subsequently reduce the boom. However, with the new reduced sun roof aperture (windows closed) the boom could be regenerated by increasing road speed, to a new higher critical speed.

2. FEEDBACK CONTROL OF FLOW OSCILLATIONS

Previous work by a number of authors has demonstrated the active control of flow-excited oscillations using the principle of feedback. A simplified block diagram of an experimental arrangement used by Sunyach and Ffowcs Williams (1986), for example, is shown in Figure 2. In this experiment the Helmholtz resonance of a cavity was excited by an external flow of air across the neck, causing a narrow band peak in the spectrum of the pressure inside the cavity at about 140 Hz, which was about 25 dB greater than the background broadband noise. By feeding back the internal pressure in the cavity to a loudspeaker inside the cavity via a fixed electronic controller, the 140 Hz peak in the spectrum of the internal pressure was reduced to the level of the broadband noise.

The action of the active controller can be modelled using a frequency domain analysis similar to that of Sunyach and Ffowcs Williams (1986). Assuming linear superposition of small amplitude variations, the complex external pressure, p_e, can be written as

$$p_e = p_t - Z_r q \tag{2.1}$$

where p_t is the external pressure due to the flow alone, Z_r is a radiation impedance, and q is the volume velocity of the flow *into* the cavity. The frequency dependence of all quantities is suppressed for notational convenience. The volume velocity drawn *from* the cavity by the loudspeaker is given by

$$q_s = Y_a p_i \tag{2.2}$$

ADAPTIVE FEEDBACK CONTROL OF SUN ROOF FLOW OSCILLATIONS

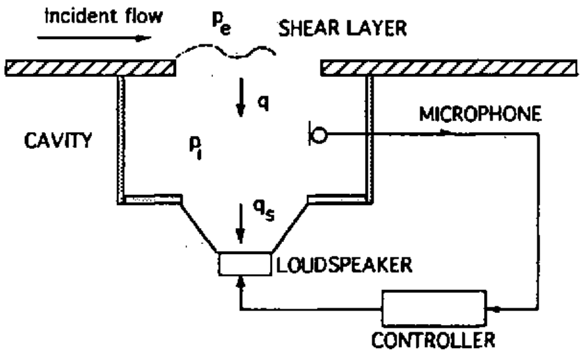

Figure 2. Simplified block diagram of the feedback control of a flow-excited cavity, after Sunyach and Ffowcs Williams (1986).

in which p_i is the internal pressure in the cavity and Y_a is the gain of the feedback control system, which has the dimensions of an acoustic admittance. The pressure is assumed to be uniform inside the cavity, and is given by

$$p_i = Z_c(q - q_s) \tag{2.3}$$

where Z_c is the impedance of the cavity which will be assumed below to be purely compliant. The final, and most important, equation is that linking the pressure differences on the two sides of the cavity neck $(p_e - p_i)$ with the volume velocity flowing through it. These quantities are assumed to be linearly related via a complex frequency dependent impedance Z_n, so that

$$p_e - p_i = Z_n q. \tag{2.4}$$

Combining equations (2.2) and (2.3), we find that

$$q = \left(\frac{1 + Z_c Y_a}{Z_c}\right) p_i. \tag{2.5}$$

Combining equations (2.1) and (2.4), we also find that

$$p_t = p_i + (Z_n + Z_r)q \tag{2.6}$$

so that, finally, using equations (2.5) and (2.6) we can see that the ratio of the complex pressure inside the cavity to that outside due to the flow is

$$\frac{p_i}{p_t} = \frac{Z_c}{Z_c + (Z_n + Z_r)(1 + Z_c Y_a)}. \tag{2.7}$$

The equivalent circuit for this lumped parameter model of the actively controlled flow excited cavity is shown in Figure 3. We now assume that the combined effect of the acoustic impedance of the neck, and radiation impedance can be represented as

$$Z_n + Z_r = j\omega L + R \tag{2.8}$$

where L is the combined acoustic inertance of the neck and radiation term and R is their total acoustic resistance. Sunyach and Ffowcs Williams discuss the fact that these quantities are dependent on the flow conditions over the neck, and note that the resistance term can become negative under certain flow conditions. Assuming also that $Z_c = 1/j\omega C$, where C is the acoustic compliance of the cavity, the ratio of pressures, equation (2.7), can then be written as

$$\frac{p_i}{p_t} = \frac{1}{1 + (j\omega L + R)(j\omega C + Y_a)}. \tag{2.9}$$

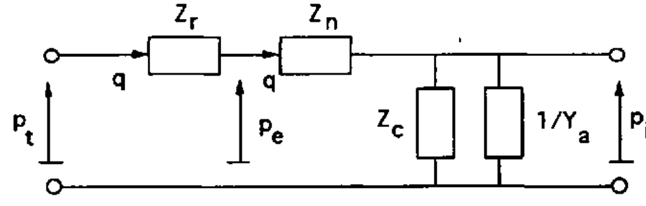

Figure 3. Block diagram of the lumped parameter model of the actively controlled flow excited cavity.

In the absence of active control, $Y_a = 0$ and equation (2.9) becomes

$$\frac{p_i}{p_t} = \frac{1}{j\omega CR + 1 - \omega^2 LC} \tag{2.10}$$

which is the standard equation of a second order resonator. Clearly, if R is negative, because of the flow, the system will be unstable and oscillate at its natural frequency $\omega_0 = \sqrt{1/LC}$. Equation (2.9) suggests a number of possible strategies for overcoming this instability. If, for example, the feedback controller included a differentiation, gain and inversion, such that $Y_a = -j\omega C$, then the natural compliance of the cavity would be removed by the active controller and p_i would become insensitive to L and R since the flow through the neck, q, would be zero, and so $p_i = p_t$. Other possible control strategies are revealed if equation (2.9) is expanded to give

$$\frac{p_i}{p_t} = \frac{1}{j\omega C(R + Y_a L/C) + (1 + Y_a R) - \omega^2 LC}. \tag{2.11}$$

By comparing equation (2.11) with (2.10), it is clear that the total "resistance" in the feedback system, $(R + Y_a L/C)$, could be made positive, even if R is negative, by ensuring that Y_a is a sufficiently large positive real constant at the frequency of interest.

In any experimental arrangement the analysis above will be considerably complicated by the frequency response of the loudspeaker, but it is clear that active control can, potentially, be achieved in a *variety* of ways. Rather than specify the mechanism of control *a priori*, by using a fixed electronic controller, it is interesting to allow the controller to be adaptive, and thus, hopefully, to find whichever controller frequency response minimises the selected error criterion.

3. ADAPTIVE CONTROLLERS

Adaptive controllers have been used successfully for *feedforward* approaches to active control for some time, with application, for example, to controlling noise in ducts (Eriksson *et al*, 1987), cars (Elliott *et al*, 1988) and aircraft (Elliott *et al*, 1990). It is far easier to change the coefficients of a digital filter adaptively than those of an analogue filter. Adaptive digital filters have also been widely studied because of their importance in other applications (Widrow and Stearns, 1985). If a finite impulse response (FIR) digital filter is used in a purely feedforward active controller, it is readily shown that the variation of the mean square residual error with any of the filter coefficients is quadratic, with a unique global minimum. The "error surface" of such a controller is thus guaranteed to be unimodal and gradient descent methods, such as the LMS algorithm (Widrow and Stearns, 1985) will thus always converge monotonically towards the optimum solution.

Gradient descent methods have also been used to adapt the coefficients in feedback controllers, even though there is no guarantee that the error surface will be unimodal under these conditions. In the 1940's a gradient descent method known as the "MIT rule" was used to adjust analogue flight controllers (Åström and Wittenmark, 1989), although such methods went out of favour after instabilities in flight! More recently, Billoud *et al* (1991) used a digital IIR filter as the feedback controller for the control of flow-excited cavity oscillations. The coefficients of the IIR filter were adjusted using the RLMS algorithm (Eriksson *et al*, 1987), which is essentially a gradient descent method. An unusual feature of the algorithm, as it was implemented here, was that the same signal (that from the internal pressure microphone) was used both as the reference signal driving the adaptive controller, and as the error signal which the adaptive controller was attempting to minimise. Billoud *et al* (1991) report reductions of about 20 dB at the peak of the internal pressure spectrum in a flow-excited cavity, which occurred at about 180 Hz in these experiments. These authors have also considered the error surface for this problem. Specifically, they have plotted the variation of mean square pressure in the cavity as the first two non-recursive filter coefficients in the feedback controller are varied. They find that no clear minimum exists in this surface but there are many combinations of the two coefficients which give similar attenuations. This is contrasted with the error surface for a well-conditioned feedforward controller, for which a clear unique minima exists, as mentioned above. The existence of this broad range of possible feedback controllers, which all suppress the oscillations of the flow excited resonance, may support the observations of Sunyach and Ffowcs Williams (1986), discussed in the previous section, that there may be a variety of control strategies which can suppress this instability. Similar error surfaces can also be observed, however, in purely feedforward control systems if the control problem is not well conditioned (Elliott *et al*, 1992). One method of improving the conditioning of such systems is to add a leak to the adaptation algorithm (Elliott *et al*, 1992), as was used in the experiments below.

The controller used in the experiments reported here was based on a duct noise control system demonstrated at ISVR in 1987. The physical components of the feedback controller, and the equivalent block diagram, are shown in Figures 4(a) and (b). In these diagrams, H(z) is the transfer function of the FIR digital control filter and G(z) is the transfer function of the "plant" under control, which in this case includes the electroacoustic response between the loudspeaker and microphone, and that of the data converters. An initial identification phase was used to adapt another digital filter, $\hat{G}(z)$, which modelled the electroacoustic response from the loudspeaker to the microphone, this was then used to filter the reference signal in the filtered-x LMS algorithm used to adapt the coefficients of H(z), as shown in Figure 4(c). If the i-th coefficient of H(z) at the n-th sample time is denoted $h_i(n)$, each of the filter coefficients was updated at every sample interval using the equation

$$h_i(n+1) = (1 - \alpha\beta)\, h_i(n) - \alpha\, e(n)\, r(n-i) \qquad (3.1)$$

where α is a convergence coefficient, β a leakage factor, e(n) the sampled error signal, and r(n) the filtered reference signal which, in this case, is obtained by passing e(n) through $\hat{G}(z)$. The sample rate of the digital filter was 3 kHz, and it was implemented to give the least possible delay from input sample to output sample. No anti-aliasing or

ADAPTIVE FEEDBACK CONTROL OF SUN ROOF FLOW OSCILLATIONS

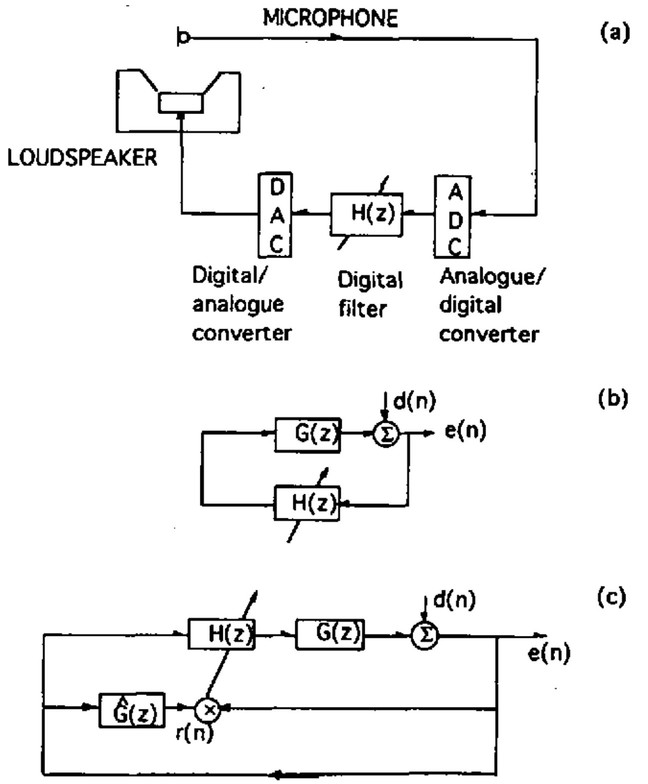

Figure 4. The physical components of the feedback controller (a) and its equivalent block diagram (b). The block diagram of the filtered-x LMS algorithm used for the adaptation of H(z) is also shown (c).

reconstruction filters were included in the feedback loop so that no delay would be added by these components. This minimisation of loop delay allows the possibility of a relatively high loop gain without instability.

Another control filter arrangement which was tried in this application was the parallel connection of a feedback filter W(z) and feedforward filter -F(z), as shown in Figure 5. Such an arrangement is widely used for echo cancellation in telecommunications and has previously been used in feedforward active control in ducts. Its use in a feedback loop is discussed by Forsythe *et al* (1991). The overall transfer function of the controller in Figure 5 thus becomes

$$H(z) = \frac{W(z)}{1 + W(z)F(z)} \qquad (3.2)$$

and the behaviour of the complete feedback loop is thus described by the equation

$$\frac{E(z)}{D(z)} = \frac{1 + W(z)F(z)}{1 - W(z)G(z) + W(z)F(z)}. \qquad (3.3)$$

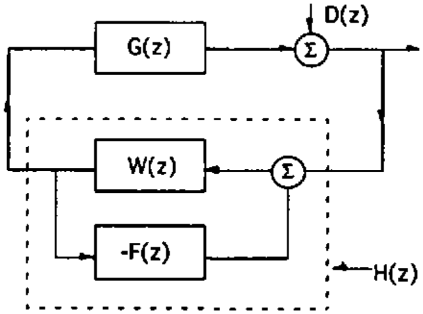

Figure 5. The feedback control loop in which the controller, H(z), is implemented as two filters in parallel to give the response H(z) = W(z)/(1 + W(z)F(z)).

If it can be arranged that F(z) is a good approximation to G(z), using for example the filter already obtained during the identification phase, then the error signal becomes

$$E(z) = (1 + W(z)G(z))D(z). \qquad (3.4)$$

The mean square error is then a quadratic function of the weights in the FIR filter W(z) and should thus be easier to adapt. In fact, if G(z) were a pure delay, the action of W(z) becomes similar to the adaptive line enhancer widely used in adaptive signal processing (Widrow and Stearns, 1985).

In the application discussed here, this filter arrangement was, however, only slightly more stable than that shown in Figure 4. This perhaps reflects the fact that the response of the system under control, G(z), changes with time, particularly as the airflow over the sunroof increases with speed. Under these conditions, the cancellation of the two terms in the denominator of equation (3.3) will not be exact, and the resulting mean square error signal will not be quadratic in the coefficients of W(z), as would be expected from equation (3.4).

4. PRACTICAL RESULTS

The filter arrangements of Figures 4 and 5 were implemented with a range of filter lengths of between 16 and 64 for both feedforward, (F(z)), and feedback, (W(z)), filters. Filter lengths of approximately 32 taps were found to give the most repeatable results. For filters longer than 32 points, it was found that the filter was prone to adapt into a state with large coefficients towards the end of the controller impulse response. Instability of the control system occurred soon after this.

The feedforward filter, F(z), was non-adaptive, after the initial identification phase, and the most stable state of the control system was found empirically to be with the coefficients of this filter set to half of that required to match the feedback path with the car stationary. The performance differences between filter lengths of between 8 and 32 coefficients were indistinguishable because of the variability in the original noise signal, caused by wind gusting.

The control system was run both with and without anti-aliasing and reconstruction filters. It was found that the delay added by these filters (~ 2-3 ms) caused the onset of instability in the controller to be far more likely. The noise suppression in the car was also far less with the anti-aliasing filters than without. Without reconstruction filters, however, considerable audible distortion resulted.

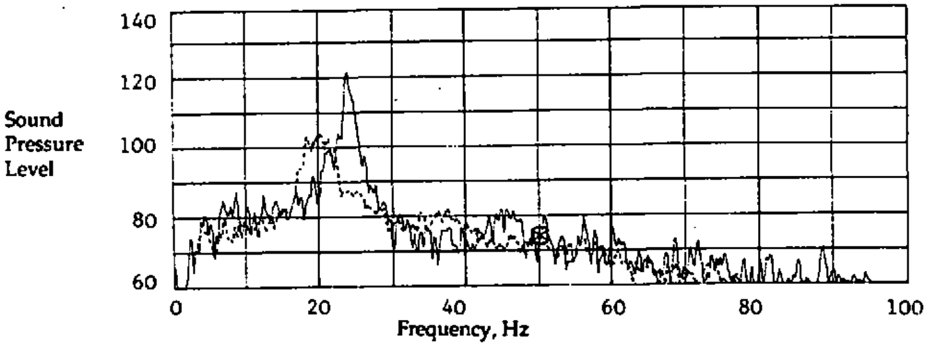

Figure 6. Sound pressure spectrum measured inside the car with (dashed) and without (solid) feedback control.

The secondary sound sources used were four 8" loudspeakers driven in parallel, using a 100 W amplifier. This was found to be barely adequate to establish control if oscillations had built up in the car prior to turning on the control system. However, if the control system was switched on prior to the acoustic oscillation reaching large levels, then the drive signals to the secondary source were found to be relatively small. The spectrum of the resulting sound pressure inside the car is shown in Figure 6, together with the spectrum with no feedback controller. The active control system has clearly reduced the tone at 25 Hz by about 30 dB, although some enhancement of the broadband noise at other frequencies can also be seen.

The impulse response of the control filter continually changed during cancellation and if adaptation of this filter was stopped while allowing control to continue, then instability frequently resulted within a few seconds. The controller was thus continually adjusting itself into stable operation.

5. CONCLUSIONS

When driving with an open sun roof at certain critical speeds, intense but very low frequency tones are often experienced in cars. The cause of these tones is the interaction between the shear layer flowing over the sun roof, and the compliance of the air volume inside the car.

Previous laboratory work has demonstrated that such flow excited oscillations can be controlled with an active control system in which the pressure in the cavity is fed back to an internal loudspeaker via an electronic controller. By using a simple theoretical analysis it can be shown that such an arrangement can suppress the oscillations in a variety of ways. We have investigted the use of adaptive digital filters as the controller for such a system implemented within the car. The most important aspect of the controller in determining the performance of the control system was found to be the overall delay in the open loop system. This was minimised by an efficient implementation of the digital control filter, and by not using analogue anti-aliasing and reconstruction filters. This does, however, cause some increase in broadband noise at higher frequencies because of aliasing, which somewhat degrades the subjective effect.

The experiments in the car demonstrated that the original peak in the sound pressure spectrum, at 25 Hz, could be reduced by up to 30 dB with the feedback controller, although the broadband noise at about 20 Hz was somewhat increased in the process. If the control system was operating while the car was driven up through the critical speed, the secondary loudspeakers were not required to operate very hard to maintain control. If, however, the flow-excited oscillation was allowed to build up before the control system was switched on, the loudspeakers had to operate quite hard to establish control. If a smaller loudspeaker were used, it may be that control would be maintained most of the time, but that if for any reason the flow-induced oscillation did build up beyond a certain point the control system would no longer be able to maintain control.

6. REFERENCES

K.J. Åström and B. Wittenmark 1989 *Adaptive Control.* Addiston-Wesley.

G. Billoud, M.A. Galland, C.H. Huu, S. Candel 1991 *Proc. Recent Advances in Active Control of Sound and Vibration, Virginia,* 95-107. Adaptive active control of instabilities.

W.K. Bodger and C.M. Jones 1964 *Proc. SAE National Automobile Week Meeting, Detroit.* Aerodynamic wind throb in passenger cars.

S.J. Elliott, I.M. Stothers, P.A. Nelson, A.M. McDonald, D.C. Quinn and T. Saunders 1988 *Proc. Inter-Noise 88, Avignon,* 989-990. The active control of engine noise inside cars.

S.J. Elliott, P.A. Nelson, I.M. Stothers and C.C. Boucher 1990 *Journal of Sound and Vibration* 140(2), 219-238. In-flight experiments on the active control of propeller-induced cabin noise.

S.J. Elliott 1992 *IEEE Transactions on Signal Processing* 40(5), 1041-1052. The behaviour of a multiple channel active control system.

L.J. Eriksson, M.C. Allie and R.A. Greiner 1987 *IEEE Trans. on Acoustics, Speech and Signal Processing* ASSP-35(4), 433-437. The selection and application of an IIR adaptive filter for use in active sound attenuation.

N.H. Fletcher and T.D. Rossing 1991 *The Physics of Musical Instruments.* Springer-Verlag

S.E. Forsythe, M.D. McCollum and A.D. McCleary 1991 *Proc. Recent Advances in Active Control of Sound and Vibration, Virginia,* 879-889. Stabilization of a digitally controlled active-isolation system.

A.R. George 1989 *Proc. AIAA 12th Aeroacoustics Conference, San Antonio,* paper 1067. Automobile aeroacoustics.

G. Lackman 1989 *Automobilitechnische Zeitschrift,* Webasto Aerovent and Frontvent - Sunroof systems for the future.

P.A. Nelson, N.A. Halliwell and P.E. Doak 1981 *Journal of Sound and Vibration* 78(1), 15-38. Fluid dynamics of a flow excited resonance, Part I: Experiment.

P.A. Nelson, N.A. Halliwell and P.E. Doak 1983 *Journal of Sound and Vibration* 98(3), 375-402. Fluid dynamics of a flow excited resonance, Part II: Flow acoustic interaction.

M. Sunyach and J.E. Ffowcs Williams 1986 *C.R. Acad. Sc. Paris* 303, Série II(12), 1085-1089. Acoustics - The active suppression of oscillation in flow-excited cavities.